An Overview of Acoustic Impedance Measurement Techniques and Future Prospects

Nandeesh Hiremath [1],*, Vaibhav Kumar [2], Nicholas Motahari [3] and Dhwanil Shukla [4]

[1] von Karman Institute for Fluid Dynamics, Waterloosesteenweg 72, B-1640 Sint-Genesius-Rode, Belgium
[2] Georgia Institute of Technology, North Ave NW, Atlanta, GA 30332, USA; vaibhavkumar@gatech.edu
[3] Harvard Business School, Harvard University, Boston, MA 02163, USA; nmotahari@mba2021.hbs.edu
[4] Indian Institute of Technology Bombay, Aerospace Engineering Main Gate Rd, IIT Area, Powai, Mumbai, Maharashtra 400076, India; dhwanil@aero.iitb.ac.in
* Correspondence: nandeesh.hiremath@vki.ac.be

Abstract: In order to progress in the area of aeroacoustics, experimental measurements are necessary. Not only are they required for engineering applications in acoustics and noise engineering, but also they are necessary for developing models of acoustic phenomenon around us. One measurement of particular importance is acoustic impedance. Acoustic Impedance is the measure of opposition of acoustical flow due to the acoustic pressure. It indicates how much sound pressure is generated by the vibration of molecules of a particular acoustic medium at a given frequency and can be a characteristic of the medium. The aim of the present paper is to give a synthetic overview of the literature on impedance measurements and to discuss the advantage and disadvantage of each measurement technique. In this work, we investigate the three main categories of impedance measurement techniques, namely reverberation chamber techniques, impedance tube techniques, and far-field techniques. Theoretical principles for each technique are provided along with a discussion on historical development and recent advancements for each technique.

Keywords: aeroacoutics; rotor acoustics; impedance; absorption coefficient; liners; bulk absorber; impedance matching; reverberation chamber; impedance tube; free field

1. Introduction

Impedance in acoustics is the measure of the opposition that a system presents to acoustic flow resulting of an acoustic pressure applied to the system. It indicates how much sound pressure is generated by the vibration of molecules of a particular acoustic medium at a given frequency. Some other widely accepted definitions based on specific applications are mentioned below [1].

- The specific acoustic impedance, z (pressure/particle speed), a characteristic property of the medium and of the type of wave that is being propagated.
- The acoustic impedance, Z (pressure/volume velocity), a term useful in discussing acoustic radiation from vibrating surfaces, and the transmission of this radiation through lumped acoustic elements or through pipes and horns.
- The radiation impedance, Zr (force/particle speed), used in calculating the coupling between acoustic waves and a driving source or driven load.

At first, impedance measurements were performed with analogue devices, where curves were plotted using values directly obtained from an analogue output signal. Most of these analogue sensors measured impedance by using a source of constant velocity, and obtaining a pressure signal using a microphone which would be approximately proportional to the impedance. However, since the mid to late 1970's, the advancement of computational methods has lead to the development of impedance measurement methods based solely on pressure measurements, which can then be used for finding the impedance

of absorbing materials or for multi-port characterization [2]. There are several techniques to determine the acoustic impedance of materials. These techniques can be divided into three groups: measurements in a reverberant room, measurements in an impedance tube and free field measurement techniques. The theory behind these broadly classified measurement types and the working principles behind different variants of measurement techniques are explored in the following sections.

Reverberation chamber works on the principle of reverberation time. It consists of a chamber with highly reflective walls, ceiling, and floor. The reverberation time of such a room is very long, and the longer it is, the more accurate the measurement. A standard sample of the material to be tested is laid on the floor and the reverberation time is measured. Comparing this time with the known reverberation time of the empty room yields the impedance of the sample material. A detailed study on reverberation chamber technique with its limitation is explored by Kosten [3]. The Impedance Tube method works on the principle of standing waves in a tube. The sample of interest is placed at one end of the tube and standing waves are generated in the tube. Based on the standing wave ratio (SWR) which is defined as the ratio between maximum/minimum pressure amplitude, and relative magnitudes of the incident and reflected waves the impedance of the sample is measured. A detailed study on tube methods with their limitations are referenced in Beranek et al. [4], Taylor et al. [5], and Zwikker et al. [6]. Often times, these methods are restricted by the underlying assumption of plane wave approximation and are limited by diffraction from edges of the sample. In most cases, these techniques are applicable for locally reactive surfaces. On the contrary, free field measurements [7] are not bounded by any physical boundaries and are not limited by any diffraction, for example impedance measurement of grass on an open field or a sample in a large room.

Figure 1 shows an overview of the existing techniques used across various domains. Primarily, the measurement techniques can be classified into pressure based and velocity based methods. The pressure-pressure coupling through single/multi microphones and multi-point microphones have been in practice over several decades. On the other hand, velocity-velocity coupling is fairly new, especially in the case of two-dimensional velocity fields from particle image velocimetry (PIV) and high temporal resolution Laser Doppler Velocimetry (LDV). In either of the two cases, a plane wave assumption must be imposed or respected in arriving at impedance. Similarly, pressure to velocity coupling or inverse coupling through modeling (Euler momentum equations) are devoid of any assumptions related to the nature of wave. The inverse coupling using PIV is one of the less explored topics and it could lead to successful determination of spatially and temporally resolved impedance characterization. Among all these methods, the fundamental distinguishing factor is the type of instrumentation/probing device used. Looking at the current trends in the machine learning and data-driven approaches to engineering problems, the future prospects might have a greater influence on acoustic impedance measurements. Based on the limited measurement data sets using limited instrumentation, a data-driven inverse problem approach could pave way to better modelling of pressure-velocity (and inverse) coupling. Data-driven methods involving supervised machine learning techniques and neural network are being used for seismic studies [8–10] and show promising research avenues. Based on the published literature, the current focus is on understanding the rock properties based on the acoustic sampling through impedance measurements. Such inverse coupling methods using data to physical/semi-empirical model approach could be generalised for other materials and applications.
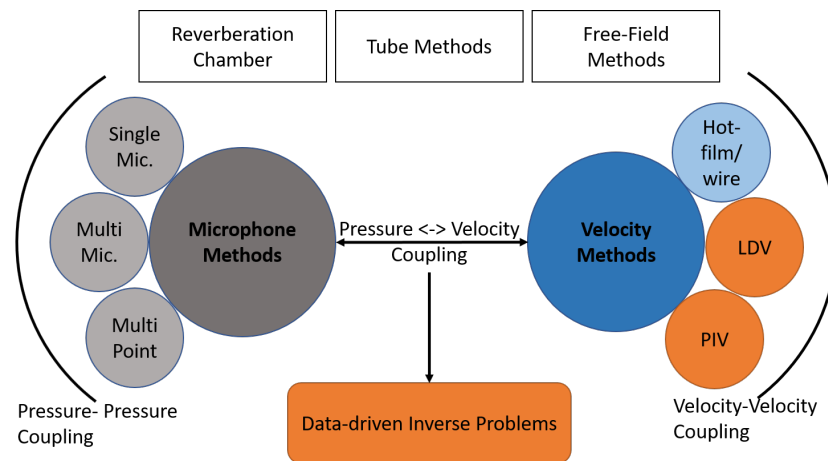
Figure 1. A schematic detailing the classification of existing methods. A data-driven approach derived from various coupling models could pave way for inverse problems.

2. Overview of Basic Formulations

Before delving into various measurement techniques, the underlying phenomena and the mathematical formulations are briefly described in this section. While the main focus is on the characteristic properties of acoustic liners and absorbers, one has to be clear about the assumptions made in acoustic wave propagation itself. By deriving similarities from light optics, the impedance of material and air can be construed as analogous to refractive indices. Just like the characteristic impedance of a material, air as a medium also has an impedance of its own. This field impedance relies on the acoustic wave propagation.

In the case of plane wave approximation, the characteristic field impedance is defined as, $Z_\circ = \rho_\circ c_\circ$ with the density $\rho_\circ$ and speed of sound $c_\circ$. For spherical waves, the characteristic impedance is given by

$$Z_\circ = \rho_\circ c_\circ \frac{ikr}{1 + ikr},\tag{1}$$

wherein 'k' is wave number, 'r' radius vector and 'i' the imaginary notation. Only for large values of 'r' compared to the wave length $\lambda = 2\pi/k$ (or kr >> 1) this characteristic impedance of a spherical wave converges to a real and constant value of $Z_\circ$ for a plane wave. And for small values of 'kr' this quantity is complex.

The balancing factors like transmission, reflection, absorption, and attenuation form the basis for acoustic energy balance. The underlying physics and the formulations described below are common to all known impedance measurement techniques. As mentioned before, the impedance of interest is the acoustic impedance, Z, which is related to the pressure, p, and the velocity, v_n, in the following way:

$$Z(\omega) = \frac{\hat{p}}{\hat{v}_n},\tag{2}$$

where $\hat{p}$ and $\hat{v}$ denote that both the pressure and velocity can be complex terms for a range of frequencies (ω [rad/s]). Considering the normal direction as the direction towards the material, at a single frequency, the pressure can be expressed as the following:

$$p = \hat{p}e^{i\omega t},\tag{3}$$

where t is time (in seconds). The velocity in the normal direction also follows a similar form:

$$v_n = \hat{v}_n e^{i\omega t}.\tag{4}$$

In case of multi-point measurements, the pressure as a function of distance x can be written in the following way:

$$\hat{p} = \hat{a}(e^{ikx} + R(\omega)e^{-ikx}), \tag{5}$$

where $\hat{a}$ is the amplitude of the pressure, k is the wave number (defined as ω/c), and R is the reflection coefficient, c is the speed of sound. Using this, and the equation of momentum, the following equation of velocity as a function of x can be derived:

$$\hat{v}_n = -\hat{v}_n = \frac{\hat{a}}{\rho_0 c_0}(e^{ikx} + R(\omega)e^{-ikx}), \tag{6}$$

where ρ_0 and c_0 are the mean density of the medium (air) and the speed of sound of the medium. Substituting Equations (5) and (6) into Equation (2) and solving for it at $x = 0$, the following relationship between impedance and the reflection coefficient is seen:

$$Z(\omega) = \frac{1 + R(\omega)}{1 - R(\omega)}. \tag{7}$$

It should also be noted that the reflection coefficient, R, is related to the absorption coefficient, α through the following equation:

$$\alpha = 1 - |R|^2. \tag{8}$$

The above formulations are limited to reflection and absorption of sound. In a similar fashion other governing factors can be added in the momentum/energy balance. With a trained eye, one could notice that the particle velocities are modeled based on the pressure fluctuations. In other words, there is an inherent one way coupling from pressure to velocity. Most of the measurement techniques described in this paper follow this conventional wisdom, wherein, crux of the techniques hovers around pressure measurements. In few cases, acoustic velocities are measured firsthand, thereby modeling the pressure by backward coupling. The specific impedance thus becomes a derived quantity. More to it, the quality of measured quantities directly affects reflection, absorption, transmission coefficients, which in turn dictate the specific impedance.

3. Reverberation Chamber Techniques

The absorption coefficient and impedance are related and oftentimes measuring one would deduce the other. In many applications, it is required to measure sound absorption characteristics of a sample when subjected to sound from arbitrary directions and of random phase relations. For doing that, measuring sound absorption at each possible orientation one at a time is extremely time consuming and expensive. Such applications do not need direction resolved measurements. This is where the reverberation chamber method of impedance measurement is useful [11]. Unlike impedance tube methods, the reverberation chamber method is not restricted to the study of behavior of a surface. Often, the whole object (or model scale) is tested to see how it absorbs sound waves. One of the most intuitive examples of why the acoustic behavior of full objects are important is the reverberation of sound in a room without furniture. Furniture takes up a lot of sound energy and reduces reverberation effects. Similarly, in hall like theaters, convention centers and so forth, objects in the hall contribute significantly to the sound quality. Other important uses of reverberation chambers are to measure overall sound power due to devices, automobiles and so forth because effects due to the directionality and spread of the noise sources are lost by arbitrary reflections from skewed walls and other reflective surfaces.

3.1. Non-Parallel Walls and Skewed Surfaces

Measuring overall absorption characteristics requires sound to approach the object from all possible directions at all possible frequencies and phases. To achieve uniformly spread direction of incidence and random phases, the reverberation chamber features non-parallel sound reflective walls and other devices which reflect off sound in arbitrary fashion. Without a test specimen, having totally reflective surfaces in reverberation chamber

would mean perpetual, non-decaying sound in the room even after the source has stopped. In presence of a specimen, the sound level would decrease with time due to sound being absorbed by the specimen. The decay time of sound indicates the rate at which specimen absorbs sound, which is used to find the absorption coefficient. Instead of measuring the overall time of sound decay, measuring Reverberation time (T_{60}), which is defined as the time taken (in seconds) by sound to drop by 60 dB of the original level, is more appropriate and reproducible. Assuming exponential decay of the sound intensity (I [W/m^2]) with respect to reference value (I_0), reverberation time can be found from experimental results using the following expression.

$$T_{60} = \frac{-at}{\ln \frac{I}{I_0}},$$ (9)

where a is the constant 13.8155 and t is the time (in seconds) between the initial and final sound intensity measurements.

An empirical relation between reverberation time and the absorption coefficients was first found by W.C Sabine [12] before 1920 which is still used for estimating reverberation time from absorption coefficients.

$$T_{60} = \frac{0.161V}{4mV + S_e},$$ (10)

where T_{60} is in seconds, V (volume of enclosure) is in m^3, and Se (effective absorbing area) is in m^2. The effective absorbing area is given by the total area of surfaces in the chamber (S) multiplied by the average absorption coefficient. Absorption coefficient, α, characterizes the ability of a material to absorb sound. Theoretically, this ranges between 0 and 1, with 0 corresponding to no sound absorption and 1 corresponding to 100% sound absorption. 'm' is the energy attenuation constant per unit length of sound travelling through air.

$$S_e = S\alpha_a$$ (11)

$$S\alpha_a = \sum \alpha_i S_i.$$ (12)

The absorption of sound by air is often neglected as it is negligible compared to the absorption by surfaces in the case of moderate sound amplitudes where propagation is still linear. Hence the term '4 mV' is dropped. The Sabine's expression assumes diffused sound field. A sound field is considered diffused if it satisfies the following conditions: (a) Sound waves are incident from all directions with equal intensity and random phase relations, at any position in the room; and (b) The reverberant sound field is the same at every position in the room. The paper by Hodgson [13] talks extensively about how well and when which version of diffuse field theory by Sabine are applicable in different chamber shapes and surface characteristics, and how they affect estimates of reverberation times and steady state sound pressure level. There are many different empirical relations developed after Sabine's which conform better to the experimental results and relax the requirement of a diffused sound field to some extent [14–18].

3.2. Wall Dimension and Material Selection

The design of a room affects how well the diffused field is achieved and thus affects the correctness of obtained results. Hence, careful design of a reverberation chamber is necessary to ensure that the room provides a large number of modal frequencies at equalized mode spacing. Some of the design variables are: shape and dimensions of the room, reflective surface material, diffusers, location and nature of sound source, microphones and their location, location of specimen, and sound insulation. The shape and dimensions of a reverberation chamber affects the modal density (Hz^{-1}), the distribution of normal frequencies, and the presence of standing waves. It is desirable to have a very high modal density for the frequencies to be measured. The volume of the reverberation chamber is dictated by the lowest frequencies that are to be measured reliably as spectral density is

function of volume and frequency. Standing waves can be prevented by ensuring that no two surfaces in the chamber are parallel to each other. The recent work by del Ray et al. [19] has shown the feasibility of having a reverberation chamber with relatively small size.

Careful selection of material to have reflective surfaces is necessary to ensure that the reverberation time of the chamber by itself is long enough. The longer reverberation times of an empty room is desirable for accurate measurements as then most of the absorption could be attributed to the specimen only and results will be less sensitive to measurement errors. Materials used in reverberation chambers usually have a very low absorption coefficient ($[O] \sim 0.01$). The absorption coefficients and their response over different frequency range for commonly used materials are available at references [20,21].

3.3. Enhanced Diffusion Effects

Just the sufficient size of the chamber and non-parallel walls do not ensure perfect sound diffusion, hence, separate devices or objects are used for randomizing the sound waves further. Schultz [22] define sound diffusion, reasons why it is important, describe how the degree of diffusion can be evaluated, and give ways by which diffusion can be achieved. Some common ways of achieving sound diffusion are static suspended diffusers, stirrers, and rigid diffusers on the wall. Each of these sound diffusing methods have benefits and limitations. Means of diffusion cause some loss in reverberation time due to absorption by the devices themselves, and hence their use is limited. In the case of stirrers, the induced currents [23] and their frequency dependency plays an important role, and such effects have been studied as a radiative problem [24]. Similarly, the effect of diffusers and their optimal diffusion conditions have been studied by Kim et al. [25]. Duanqi et al. [26] placed reinforced concrete spherical diffusers of different sizes on the walls as seen in Figure 2 to ensure diffusion without causing significant reduction in reverberation time. Figure 3 shows a typical stationary suspended diffuser and a stirrer in a reverberation chamber. Hengyi et al. [27], Wanderliner et al. [28], and Zhao et al. [29] have shown an innovative method with complete departure from mechanical stirrers. They show the application of meta material coating with a random 1-bit rotating meta surface. This method has shown credible results when compared to the conventional mechanical reverberation chambers.
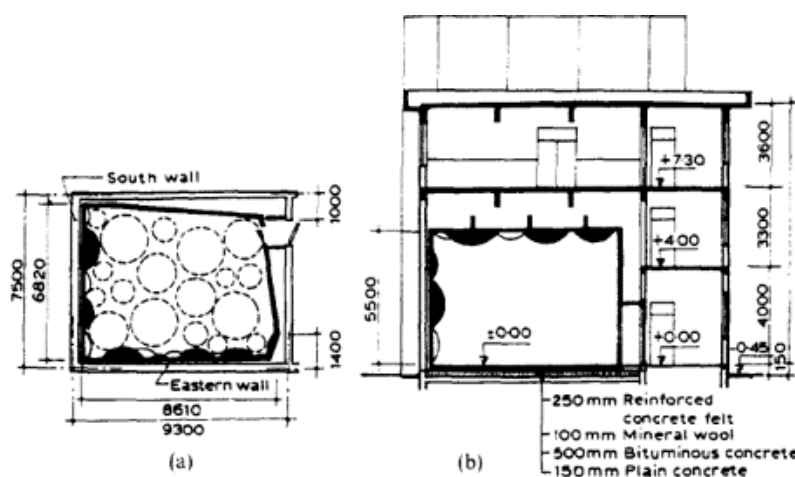

Figure 2. (**a**) Plan and (**b**) cross section views of reverberation chamber designed by Duanqi et al. [26].

Figure 3. (**Left**) Diffusers in reverberation chamber (ETS Lindgren Company, Cedar Park, TX, USA) (**Right**) Stirrer in reverberation chamber (Ecotone Systems Pvt. Ltd., Greater Noida, Uttar Pradesh, India).

Sound sources used in reverberation chambers are generally capable of emitting broad ranges of frequencies. More than one sound sources, each placed at different locations, are used for further randomizing the sound. These speakers are often mounted on suspended diffusers or rotating stirrers. ISO 3741 [30] specifies the number of speakers and number of microphones required for a given size of reverberation chamber. The ISO standard also specifies minimum distances between the microphones, distances of microphones from the noise source and the distance of microphones from walls and other surfaces. The sample to be tested is generally kept away from the walls and other devices in the chamber.

Just like for an anechoic chamber, it is necessary to limit the background noise in a reverberation chamber. Background noise dictates the extent up to which the decaying sound can be recorded and be used reliably. It is an important consideration even in case the reverberation chamber is being used to measure overall sound pressure level (OASPL-dB) of a device as the background noise would just add to the devices noise and contaminate measurements. Many techniques similar to those used for anechoic chambers are used to isolate the reverberation chamber from the external noise.

In actual reverberation time measurements, readings from all the microphones in the chamber are averaged and Equation (10) is used. Reverberation time due to an empty reverberation chamber is used to measure the overall sound absorption area of the chamber, which is subtracted out of the absorption area obtained from reverberation time with the sample in the chamber using Sabine's expression (or other more accurate empirical expressions [31]), giving absorption area of the sample. For the case of at surface samples, this absorption area divided by actual area of the sample gives the absorption coefficient of the sample's surface. These coefficients are different for different frequency sounds. Almost all materials have higher absorption coefficients for high frequencies compared to low frequencies.

3.4. White Noise vs. Tone Bursts

Since empirical relation given by Sabine for reverberation time and sound absorption coefficient, there have been many studies, improvement in theories and empirical relations. There have been advancements in sound generation devices, studies on placement of sound sources and microphones signal processing.

Traditionally, for reverberation time measurement, a continuous white noise source is used which is kept on till the sound pressure level in the room comes to a steady state. However, this approach leads to random fluctuations in decay curves because the exact form of the random fluctuations depend on the initial amplitudes and phase angle of the normal modes at the moment the excitation signal is turned off. In order to get a high amplitude sound, Willardson et al. [32] have proposed a signal processing time reversal technique wherein, the high amplitude signal is created by intentional sound focusing. Because the tests have to be done many times to average out the effects, Schroeder's [33] method can be an alternative. He came up with tone bursts method (impulse sound) to

excite the enclosure. This method could give the ensemble average of decay curves in a single measurement by simple integration over the tone burst response of the chamber.

3.5. Blind Estimation and Energy Methods

All the methods described till now for absorption coefficient computation require a known sound source. Recent development in signal processing and system identification has made it possible to estimate reverberation time in an enclosure without using a specific noise source and without any prior knowledge of the sound sources in a room [34]. This has been termed as "Blind Estimation" of reverberation time. Another approach of using total and kinetic energy (particle velocity magnitudes) densities instead of potential energy (pressure fluctuation magnitude) density has been proposed to reduce uncertainty in sound absorption, sound power measurements in reverberation chamber [35]. It is claimed that total and kinetic energy densities exhibit much greater spatial uniformity at most frequencies than potential energy density, requiring fewer sound receiver positions to produce reliable results. This approach can also potentially reduce the minimum frequency up to which a reverberation chamber can be used for measurements. Extensive current research on reverberation chamber methods for the field of electromagnetism gives opportunity to study if some of the findings or approaches can be applied in the field of acoustics too. For instance, the genetic algorithm based stirrer design optimization done for electromagnetism reverberation chamber [36] can serve as motivation to do similar design study for acoustic reverberation chamber stirrer.

4. Impedance Tube Methods

When a sound wave travelling in one direction encounters sound absorbent material, or, in general, a change in impedance, it cannot propagate without being changed. Among many possible wave phenomena that may occur in this scenario, the one having the most practical importance in an impedance tube measurement is reflection. In an impedance tube, with the acoustic driver at one end and the sample at the other, both the incident and the reflected sound waves components are superimposed in space. Therefore, only a resultant wave, formed by the superimposition of the incident and reflected wave, is measurable. Typically, the measurement is restricted to sound pressure level measurement. Thus, only a resultant sound pressure level in space is measurable. As the resultant sound pressure wave, a superimposition of the incident and the reflected sound wave, is a result of the change in medium impedance, as experienced by the sound wave, a reconstruction of pressure distribution in space can give a measure of the impedance of the sample. There are different ways of reconstructing the pressure distribution in space using point measurements of temporal acoustic pressure, some of which are described below.

4.1. Microphone Methods

4.1.1. Single Microphone Method (SMM)

The single microphone method, utilizes a single microphone for reconstruction of spatial pressure distribution. Essentially, the SMM references the measured signal at two different locations back to the signal source, instead of a reference microphone placed at another location in the acoustic wave field [37]. This technique requires mechanical movement of the microphone between two chosen locations. The SMM is thus, a tedious time consuming technique. The accuracy is limited by standing wave ratio (SWR) and the null location resolution. A potential advantage for the SMM is for impedance measurement at high frequencies, where small diameter impedance tubes are required. Due to the small size of the tube, judicious spacing of multiple microphones for the Two Microphone Method (TMM) and the Multipoint Method (MPM) is not possible. Additionally, the SMM can be implemented in measurement environments, where two or more microphones cannot be used. An excellent example of such an environment is a high temperature impedance measurement facility where the microphone can be used in the test environment for only

short periods of time. Fahy [38] and Chu [39,40] provide a detailed description of the single-microphone method.

4.1.2. Two Microphone Method (SMM)

The development of enhanced computation capabilities and fast Fourier transform algorithms fostered the advent of new impedance measurement techniques. A number of early alternatives to the SMM technique have been proposed and summarized by Singh [41]. Of particular interest to impedance measurements of acoustic materials has been the two microphone transfer method introduced by Seybert and Ross [42] and further developed by Chung and Blaser [43,44]. In the original implementation of the TMM, two fixed microphones are flush mounted on the wall of a normal incidence acoustic impedance tube. The TMM uses the ratio of complex acoustic pressures measured at two locations to model a 1-D acoustic standing wave in a deterministic fashion. The complex acoustic pressures obtained are caused by the interference of the incident and reflected acoustic waves at the face/incident plane of the test specimen. The TMM requires no movement of microphones (unlike the single microphone method) and data can thus be acquired with no reconfiguration in a short period of time. In addition to using discrete tones for excitation, this method can also be implemented with random noise excitation such as white noise which reduces data acquisition time tremendously. It is important to note that the Two Microphone Method requires very precise transfer function measurements, which requires accurate amplitude and phase calibrations for the microphones. Chung and Blaser [44] present a novel microphone switching technique to reduce calibration time for the microphones. It is also crucial to note that the two microphone method is subject to large errors when the separation distance between the microphones is half the wavelength of the test frequency.

The experimental apparatus consists of a hollow tube, typically cylindrical, with a test sample holder at one end and a sound source at the other. The sound source is connected to an amplifier which is connected to a waveform generator that generates the broadband noise. Microphone ports are flush mounted at two locations along the wall of the tube. A sample schematic of the impedance tube setup is shown in Figure 4 below. It must be noted that the tube methods have been refined over the past several decades and the schematic shown here is a very generic setup. The most recent designs in compliance with ISO standards can be referred to the works [45,46]. The work by Niresh et al. [47] provides insights into recent developments on error corrections.
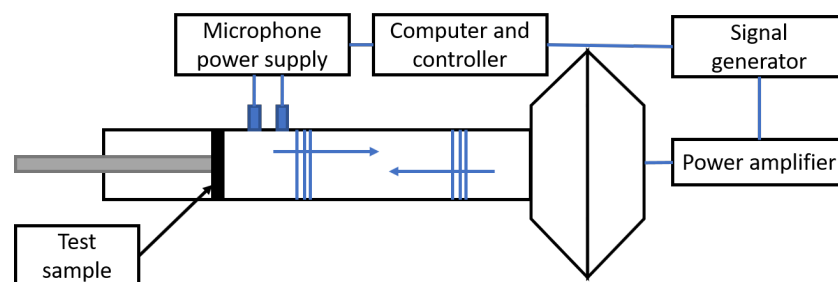

Figure 4. Instrumentation schematic for the impedance tube setup.

4.1.3. Multipoint Method (MPM)

As discussed in the previous section, temporal information of the state variable (pressure) at two locations in space is necessary for deconstructing the pressure field in the 1-D tube. In this context, analytically, the single microphone method (SMM) and the two microphone method (TMM) are deterministic methods. However, it is apparent that multiple pressure measurements in space can be used to reconstruct the best-fitted pressure distribution in the least squares.

The multipoint method involves three or more point measurements in space. The MPM is an overdetermined system.The TMM and SMM fit a wave propagation model to three or

more point measurements by employing a weighted residual technique which reduces the inaccuracies and systematic errors. This method of best-fit was first proposed by Fujimori et al. [48]. A commonly used wave propagation model, used for the MPM, was developed by Jones and Parrott [49]. The wave propagation model allowed for wall absorption and mean flow effects. As used in the Flow Impedance Test Laboratory at NASA Langley, the MPM uses complex acoustic pressure data acquired at six equally spaced measurement locations, with the spacing based on the wavelength of the selected test frequency [37]. The work by Cheung et al. [50] further provide details on the experimental reconstruction of the pressure pattern.

4.2. Direct Velocity Sensors

Two Anemometers Impedance Measurement Technique

The Microflown (p-u probe) is a unique acoustic sensor which directly measures the particle velocity instead of the sound pressure. The working principle of the Microflown is similar to a hot-wire anemometer. While a typical anemometer uses heated, extremely thin wire, the Microflown uses two thin wires [51]. The Microflown's measurements are based on the temperature difference between the two, thin, resistive wires which are few μm apart. A diagram of this setup is shown in Figure 5. A travelling acoustic wave is accompanied by movement of air. This movement of air and its interaction with the Microflown leads to heat being convected from the first wire to the second. The difference in temperature results in a difference in electrical resistance which can be measured. The difference in resistance provides a broadband linear signal that is proportional to the particle velocity up to sound levels of 135 dB. In order to insure temperatures are high enough to get a measurable temperature difference, a DC current is used to keep the operating temperature of the two wires at 400–600 K. A typical experimental setup is shown in Figure 6.
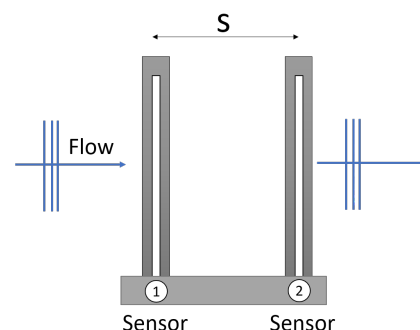

Figure 5. Acoustic flow passing over the Microflown's two thin resistive wires.
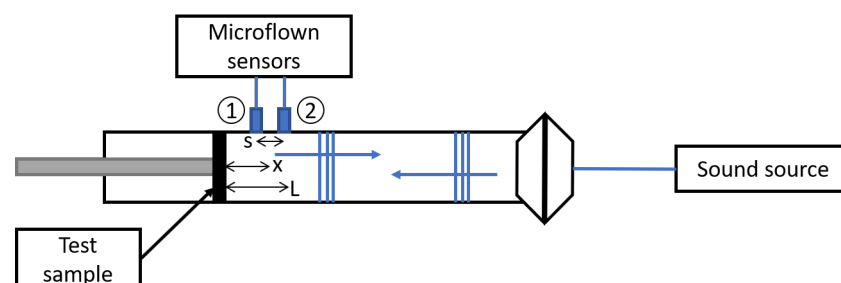

Figure 6. Impedance tube schematic using two Microflown sensors.

In order to find the reflection coefficient, the transfer function between the two Microflown sensors must be found. This is done by taking the ratio of the two Microflowns signals, or in other words, the ratio of the two measured particle velocities. Since one

sensor, based on Figure 6, is located at x = L and the other at x = L-s from the sample, the following transfer function is found:

$$H_{12}(\omega) = \frac{v_2}{v_1} = \frac{e^{ik(L-s)} - R(\omega)e^{-ik(L-s)}}{e^{ikL} - R(\omega)e^{-ikL}}. \tag{13}$$

Once the two measured velocities have been used to find the transfer function, Equation (13) shown above, can be rewritten in the following form to find the reflection coefficient as a function of frequency:

$$R(\omega) = \frac{e^{ik(L-s)} - H_{12}e^{ikL}}{e^{-ik(L-s)} - H_{12}e^{-ikL}}. \tag{14}$$

Once the reflection coefficient has been found, it can be plugged back into the previous equations to solve for the impedance and absorption coefficient. It can also be seen from the previous equations, that for a rigid termination of a tube, the impedance at a distance L is:

$$Z_L = \frac{\hat{p}(x = L)}{\hat{v}(x = L)} = \frac{\rho_0 c_0}{tanh(ikL)}. \tag{15}$$

5. Free Field Measurement Techniques

The major advantages of free field techniques, unlike impedance tube methods are that they are less impacted by the adverse boundary conditions, while taking into account for oblique incidence angles. Several techniques for impedance measurements in the free field are available in the literature. Lanoye et al. [7] provides a broader classification of the measurement techniques based on the underlying principles; (a) one, two and three microphone methods depending on one, two, and three point measurements, (b) grazing incidence and (c) sensor for particle velocity with the microphone.

5.1. Oblique Incidence Technique

Unlike normal incidence techniques that are typically implemented in impedance tubes, the oblique incidence method covers broader applications. For all measurement and theoretical purposes, high frequency waves are construed to exhibit specular reflection. The acoustic pressure field can be mapped by considering series of incident and reflected waves. The phase and amplitude maps thus obtained would provide information about the impedance of the material. Depending on the incidence angle and the frequency, the test sample of interest can act as a locally reacting or non-reacting material.

A method requiring free field conditions using specular reflection and phase difference is proposed by Ingärd and Bolt [52]. They considered a large surface area to create a pattern of interference map. The complex impedance based scheme for the analysis of such large domains by Cremer [53] was further implemented by Ando [54] with his own apparatus. It involved with the assumption of a local point source and microphone probing was done to explore the interference pattern. In order to achieve better signal to noise ratio, the experiments were performed in an anechoic facility simulating free field conditions. Later, it was noted by Sides and Mullholland [55,56] that such a technique resulted in different reactive performance. The tests on Rocksil material showed an extended reaction at 200 Hz and for higher frequencies in around 2000 Hz, it behaved as locally reacting.

If one observes the direct and reflected waves on an oscilloscope, the two signals would be time shifted corresponding to the geometric path difference traversed by the waves. Kintsl [57] used this technique to record the incident and reflected waves using a pulsed sound source and oscilloscope. Further deducing the absorption coefficient through frequency domain analysis of the recorded signals. In mathematical terms, the impedance term consists of real term indicative of resistance and the complex term indicative of frequency content. In the absence of rigorous interference pattern mapping, one could simply resort to deducing absorption coefficient by relying purely on the magnitudes of the

waves. Yuzawa [58] used an innovative method by placing two microphones equidistant from the sound source, with one microphone flushed to the test sample. By algebraically adding these two signals, the influence of the direct wave on the flushed microphone could be cancelled. Under carefully performed experiments, each microphone would ideally read pure direct and pure reflected waves respectively, thus the reflection coefficient and absorption coefficient can be deduced. To avoid unintended reflections from the distant objects, tone bursts lasting few milliseconds were used for in-situ characterization of absorption coefficients up to 70 degrees of oblique incidence angles. Hollin and Jones [59] used a similar correlation technique by cancelling the 'acoustic image' of the sound source and accounting for directivity. They provide exhaustive data sets of various materials at oblique incidence. Richard et al. [60] have shown accurate reconstruction of acoustic field for up to 60 degrees of incidence angles over a range of frequencies from 200–4000 Hz.

5.2. Extension of Microphone Methods in Free Field Environment

Holistically, microphones measure pressure fluctuations and as described in the prior sections, the method to deduce velocity term is what differentiates various techniques. In-situ impedance measurements can be very beneficial wherein the key parameter of interest, volume velocity can be directly characterized or assumed. Dalmont [2,61] and Benade [62] show exhaustive list of methods for deducing volume velocity. Among various others, velocity-servo magnetic drive, ionophone driven impedance head, and Merhaut impedance head are discussed here because of their uniqueness. In a velocity-servo magnetic drive, the sound source membrane is actuated by a servo mechanism. As the pressure waves are channeled into a tube (or free field), the volume velocity is directly deduced by the constant flow set by the servo mechanism. A slight variant of this is by using a piston to create constant flow velocity into a channel. This translational velocity of the piston is derived by the electromotive force by a current carrying coil.

An ionophone driven impedance head is unique in its own way. Unlike relying on mechanical parts for deducing volume velocity, the ionophone uses corona discharge from two closely spaced electrodes. The transducer formed by two electrodes can be considered as a microphone. What makes it unique is that the volume velocity set by the electrodes is well defined. By modulating the electrode voltage with acoustic frequencies, this can be a good compact technique. On the same principles, Merhaut impedance head uses a condenser microphone for deducing the volume velocity. A condenser microphone is placed in proximity to a flow generating diaphragm. The time derivative of the measured signal by the microphone is indicative of the volume velocity.

5.2.1. Transmission Method Using Baffled Tube

The balancing action between reflection, absorption and transmission of the acoustic waves is the essence of impedance measurements. In parallel to the discussion carried so far based on the reflected waves and interference mapping, some researchers have focused on the transmission coefficients. Starting with a plane wave assumption as observed in impedance tube methods, researchers have used the same setup for measuring transmission coefficient. The work published by Amedin et al. [63] show such a technique for free field applications. As shown in Figure 7, the setup consists of a baffled tube with sound source on one end. On the other end, a test sample is flushed to the baffle plate. Two microphones A and B capture the phase and amplitude of the incident wave and the third microphone C, located in free field measures the transmitted pressure waves. Considering the well established theories for impedance tube techniques, this method is simple to implement within the limitations of plane wave approximation. Further on, Ren et al. [64] and Takahashi et al. [65] measured the frequency dependant complex impedance using transfer function between signals of two microphones placed or two side of the porous medium.
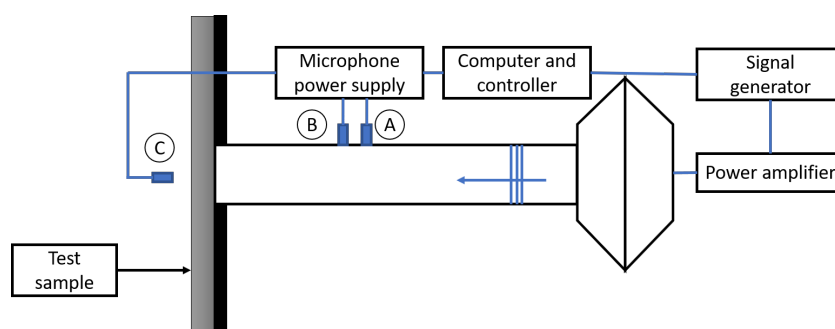
Figure 7. Block diagram showing microphone placement relative to sample and baffle.

5.2.2. Extension of One Microphone Method

The interference patterns generated by the direct and reflected waves can be complex. One scenario is to establish a standing wave pattern between the sound source and the test sample. By determining the intensity maxima and minima with their relative positions, one could retrieve the impedance. Dickinson [66] proposed one microphone method wherein, a microphone was traversed in the direction of sound propagation. As shown in Figure 8, the test sample was placed on the ground and the microphone was traversed using a cable-pulley system. The standing wave pattern was the main aspect for this study. As there is no restrictions place on the test sample, it remains undisturbed. This technique is particularly suitable for impedance characterization of large fields and outdoor spaces. Such large scale test samples in the free field environment were substantially studied by Embleton et al. [67]. In their work, they show resistivity of ground surfaces for various conditions like snow, gravel, and sand.
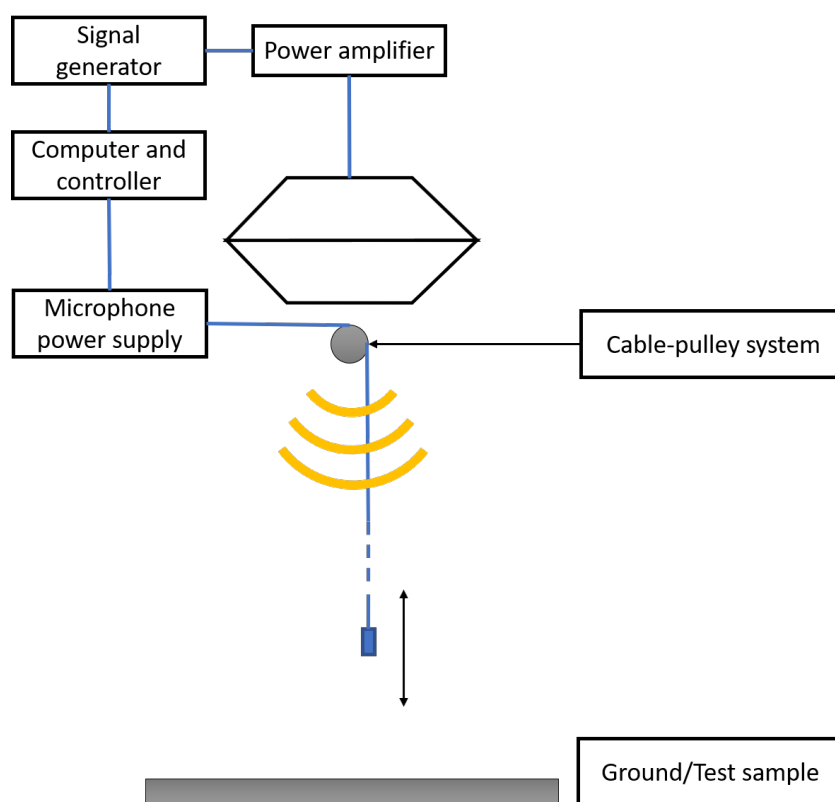

Figure 8. Apparatus for free field measurement of ground impedance using single microphone method.

5.2.3. Intensity Meters

From the first principles, sound intensity is time average of product pair of pressure and velocity. Intensity meters make use of this principle by simultaneously measuring the pressure and velocity fluctuations there by characterising the energy field. In practice this is achieved by two distinct methods. As discussed in the case of two anemometers technique, the first technique separately measures pressure and velocity with the so called p-u probes. In the second method, with the p-p probes, the pressure field is captured by pure pressure measurements. The velocity is determined by using Euler-momentum equation and the measured pressure gradient. This method mandates more than one pressure sensor.

Allard et al. [68–77], from 1985–2003, have shown the use of the two microphone method. Champoux et al. [78,79] followed the two microphones method for low frequency (200 Hz) measurements at normal incidence and demonstrated the need for pure tone signals for better precision. Further, Allard and Aknine [73] extended their work to three microphones. As shown in Figure 9, with optimal spacing between the test sample and sound source, the microphones were aligned perpendicular to the test sample and mapping was performed at discrete locations. They noted that due to finite dimensions, it was not possible to perform measurements in the whole range of acoustic frequencies. The method was further used on plastic foam with a high resistivity at oblique incidence [71] and at grazing incidence for locally non-reacting surface [77].
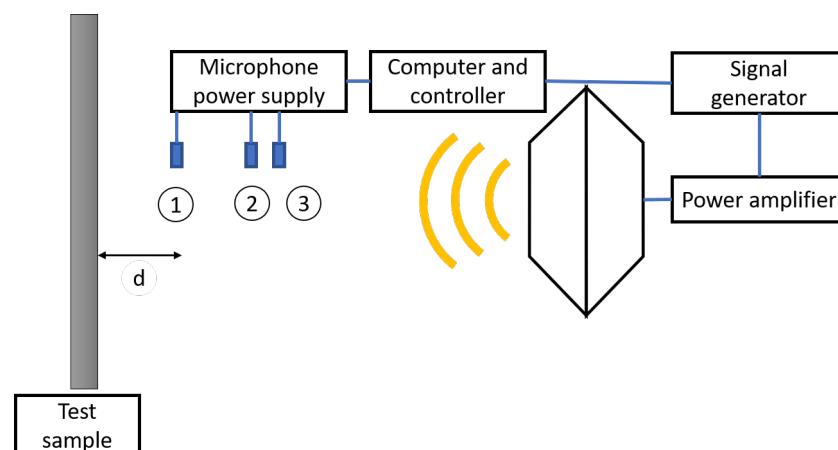

Figure 9. Sketch of the intensity meter probe with three microphones placed relative to the test sample.

5.2.4. Indirect Method Using p-p Probes

By comparative analysis of the interference pattern observed on a test sample to a reflective surface, one could assess the amount of acoustic energy absorbed by the sample. In the indirect method, a comparison for impedance is derived in juxtaposition to a highly reflective surface. Ingärd et al. [52] shows a setup using a vertically spaced microphone from the test sample. The phase and magnitude of the incident and reflected waves were compared to that of a reflective surface, thus indicating the impedance values. There is however a limitation on the characteristic dimension of the test sample as dictated by the tortuosity and characteristic viscous dimension, and is further explained by Lafarge et al. [80]. Howorth et al. [81] has contributed using similar technique, but with two microphones.

5.2.5. Phase Difference Technique

The complex impedance term consists of a real part that determines the resistance and the frequency dependant imaginary part. The spatially observed phase angle can be mapped for discrete spatial locations. Daigle et al. [82] showed the dependence of the phase angle for varying heights from a test sample. Using two microphones and a point

source, the magnitude and phase of the reflection coefficient was mapped along vertical distance as shown in Figure 10.

$$Rp = |Rp|exp^{i\theta} \tag{16}$$

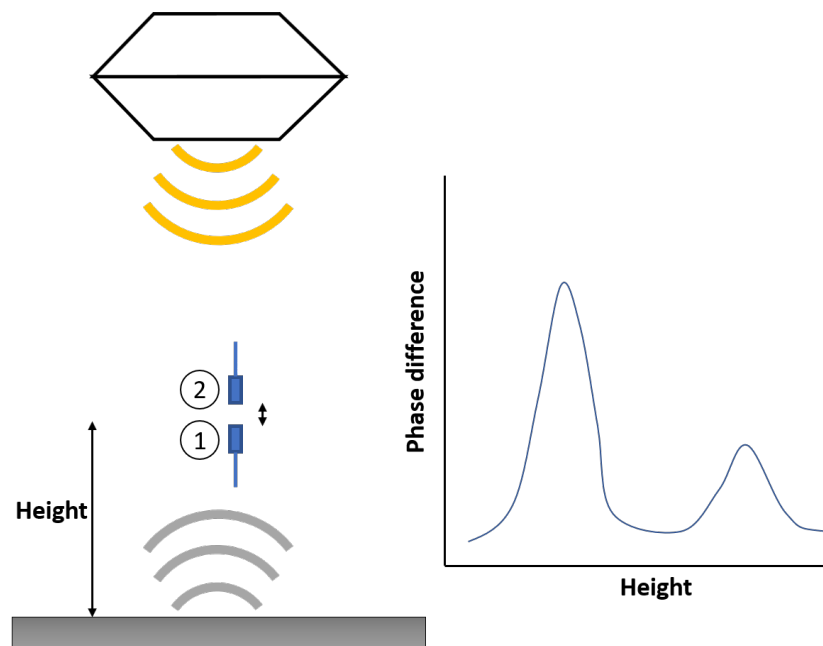$$\frac{Z}{\rho_\circ c_\circ} = \frac{1 + Rp}{1 - Rp}. \tag{17}$$

Figure 10. (**Left**) A point source at a height above the ground with two traversing receivers. (**Right**) Phase difference as a function of height for given $|Rp|$ and phase θ of reflection coefficient.

Similar to obtaining the absolute phase angle, the work by Legouis et al. [83], shows a technique based on a phase gradient normal to the test sample. Furstoss et al. [84] and Guicking [85] adapted two microphone technique at low frequency range with minimal interference on the test sample. Glaretas [86,87] used a transfer function method using two microphones, wherein the ratio of two signals was equal to the deduced velocity potentials predicted by wave propagation theory.

5.2.6. $\lambda/4$ Resonance Absorber

Furtstoss et al. [84] further showed the influence of porous layer on impedance measurements at lower frequencies. At low frequencies, the viscous forces dominate over the inertial ones. The acoustic behaviour is observed by canceling the reflected wave. As shown in Figure 11, a steady pressure drop $\Delta P = P_2 - P_1$ across a porous layer of thickness 'd' induces a steady flow of air speed 'V', and the flow resistivity is given by:

$$\sigma = \frac{\Delta P}{Vd}. \tag{18}$$

Thus, if the porous layer is placed at a quarter of wavelength from rigid impervious wall, the back pressure vanishes, and the layer input impedance can be approximated by the flow resistance
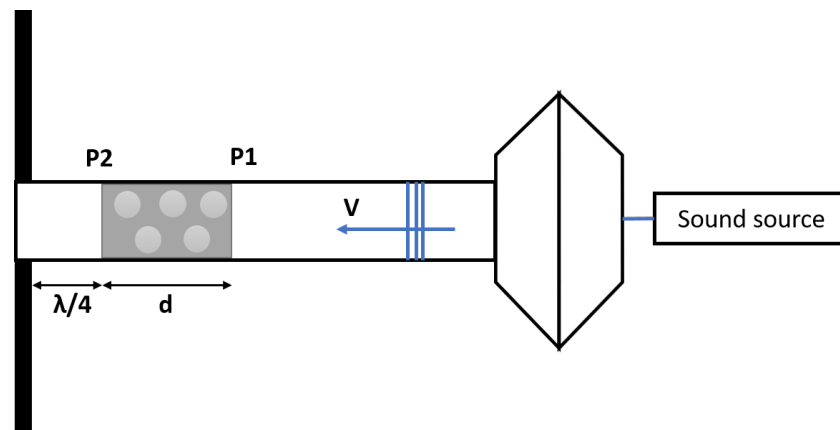
$$\frac{P_2}{V} = \sigma d. \tag{19}$$

Figure 11. Quarter wavelength technique on porous layer of thickness 'd' in a steady flow of air speed 'V'.

5.2.7. Subtraction Technique

Similar to the back pressure cancellation, Mommertz et al. [88] showed a method of measuring the complex reflection coefficient for in-situ applications. From the impulse response measured, the direct sound is cancelled by subtraction with previously obtained pseudo free field response. On a similar note, Sugahara et al. [89] have shown a filtering process using phononic crystals and phase cancellation method to remove pseudo sound.

5.3. Grazing Incidence Technique

As described in the works of Lanoye et al. [7], the theory based on the Wey-Vanderpol equation is found to be suitable for locally reacting surfaces. In other words, for liners of finite thickness. In the case of non-reacting surfaces, a similar theory exists limited to grazing incidence angle. Grazing incidence is an instance when the reflected wave grazes along the liner surface. Nocke et al. [90–92] (1997–2002) have used the grazing incidence method to characterize surface impedance. It uses a technique based on excess attenuation derived from the classical sound propagation theory to fit complex surface impedance.

The ratio of total sound field to the direct component of the sound field, termed as the excess attenuation, describes the sound pressures with and without a reflecting plane. In the method developed by Nocke, a specular reflection is assumed as shown in Figure 12 with a point source above the impedance plane, and $\pi/2 - \theta$ as the grazing angle. This method is suitable in an outdoor environment with low turbulence levels. Initially, the free field impulse response of the point source is measured by raising the source and receiver to a sufficient height above the plane for the ground reflected wave to be clearly separated in the received signal. In order to have a free field measurement, the ground reflection is removed by windowing the time signal. Then the impulse response is measured at grazing incidence above the impedance plane. The same time window is applied to this measurement while retaining both direct and ground reflected waves. The excess attenuation coefficient is thus deduced leading to impedance characterization. It must be noted that the grazing incidence technique is discussed under free field methods due to its major applicability, however, Auregan et al. [93,94] have shown such a method on quarter wavelength liners using impedance tube methods.
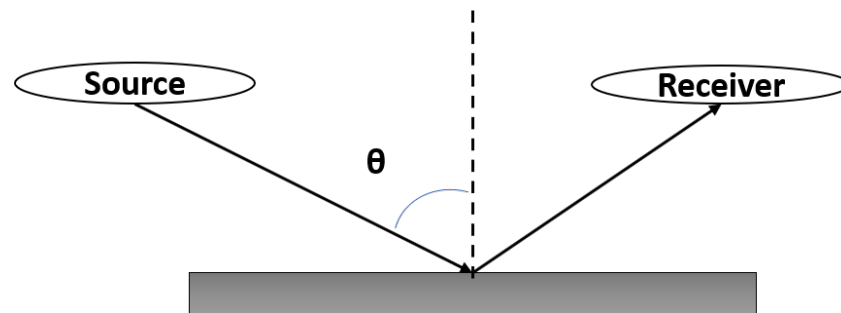
Figure 12. Configuration showing source and receiver for near specular reflection under grazing incidence technique.

5.4. Direct Velocity Sensors in Free Field

As described in Section 4, the p-u probes also find their applications in free field impedance measurements. Bianco et al. [95] and Praticò et al. [96] show the specific applications of p-u probes in free field environment. Few other direct velocity sensors specific to free field techniques are discussed here.

5.4.1. Helmholtz Resonator

Following the discussion on microphone methods in prior sections, there are mechanical ways of producing acoustic velocities. In the year 1983, Allan [97] developed a method to measure impedance of large surfaces, like ground itself. As shown in Figure 13, the setup consisted of a Helmholtz resonator. In a Helmholtz resonator, the throat diameter, throat length, and the cavity diameter are the key aspects in setting up resonance. A driven piston would set up volume velocity which is in turn measured from the piston position. The impedance is measured by further obtaining pressure signals from a microphone. The downside of this method is limitation on frequency ranges due to physical limitation of the chamber size.
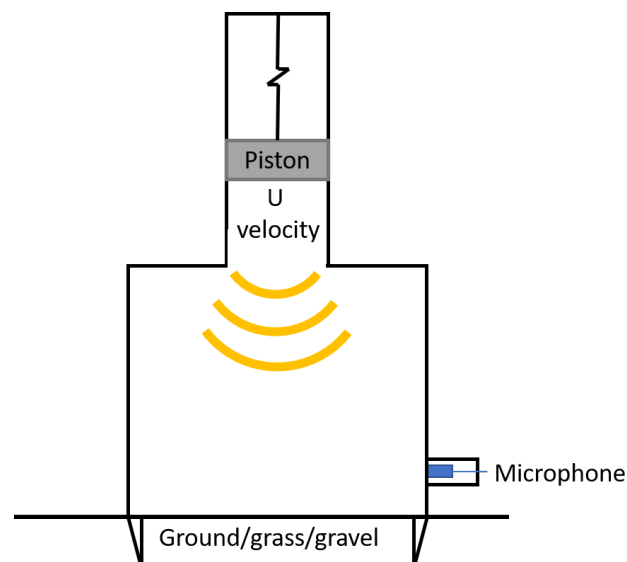

Figure 13. The volume velocity source and chamber mounted on the knife edge.

5.4.2. Near Field Acoustic Holography

Acoustic holography is a method of creating the desired acoustic field using a hologram of definite pattern. The hologram designing comprises of varying thickness substrates, thus altering the path traversed by an acoustic wave. Traditionally holographic methods have been implemented using sound pressure measurements followed by a pressure-velocity coupling. Jacobsen et al. [98,99] have shown a technique that utilises the existing velocity meters like Microflown to form a backward coupling from velocity to pressure.

They showed that such a backward coupling has better spatial resolution with higher dynamic range as the high spatial frequency components were inversely proportional to the wave number. In addition, such backward coupling was found to be less sensitive to the transducer imperfections. By using such a technique with acoustic hologram, a known geometric interference pattern can be mapped and coupled with pressure to obtain impedance. Hald et al. [100] have used microphone method in conjunction with holography technique. They use an in-situ double array microphone with Statistically Optimised Near-field Acoustical Holography (SONAH) wherein, the surface pressure and velocity are deduced, thus impedance and absorption coefficient.

6. Future Prospects

In the case of tube measurement, the conventional wisdom is limited to plane wave assumption with linearized theories. The deviations from these models are typically attributed to viscous losses. Renou et al. [101] have shown the failure of Ingard-Myers model in the presence of boundary layer. The acoustic behavior due to non-uniform velocity profile vastly deviates from the uniform flow assumptions. In addition to designing a suitable measurement technique, the future prospects vastly lies on revisiting the linearized models to better capture the viscous effects. Such effects have been vastly studied for acoustic liners [102,103] with specific applications to aircrafts. These studies have been limited to quarter wavelength resonators of uniform dimensions. The future prospects lie in generalizing such techniques for multi-layered liners and bulk absorbers with intricate porosity. Berardi et al. [104] and Iannace et al. [105] have shown studies on natural materials like grass, cork, strawand so forth. The study vastly relies on plane wave assumption with improvements made on computational algorithms. The impedance matching studies by Liu et al. [106] have shown a new approach specific to oblique incidence angles for 1D and 2D flow fields.

It is evident from the recent works that the focus has been towards improving the computational algorithms or fine tuning the conventional wisdom. These conventional methods have found applications in various areas ranging from acoustic imaging for medical applications to aircraft cabin noise reduction. In the recent years, external/internal noise reduction has gained traction with the increasing market focus towards urban air transport or flying car concepts. The need for improved measurement techniques for impedance characterisation can only increase going forward. With the advancement of high speed imaging systems, particle image velocimetry is a potential area for impedance characterization.

Extending the p-u probe technique with more spatial resolution is one possible method. Laser Doppler Velocimetry (LDV) [107] could be an alternative for hot-wire anemometers. Further, Micro-Stereo Particle Image Velocimetry technique with high-speed cameras could be used to capture acoustic velocity field. Pressure field from this 3D velocity field can further be extracted. Merkl et al. [108] have developed a pressure extraction technique for vortex dominated flow field. Such a method with the time-resolved 3D velocity field would provide a pressure field, hence a spatially and temporally resolved impedance field. In addition, further improvements in numerical schemes with backward coupling from velocity to pressure/density are some of the prospects going forward.

References

1. Kinsler, L.E.; Frey, A.R.; Coppens, A.B.; Sanders, J.V. *Fundamentals of Acoustics*; John wiley & Sons: Hoboken, NJ, USA, 1999.
2. Dalmont, J.P. Acoustic impedance measurement, Part I: A review. *J. Sound Vib.* **2001**, *243*, 427–439. [CrossRef]
3. Kosten, C. International comparison measurements in the reverberation room. *Acta Acust. United Acust.* **1960**, *10*, 400–411.
4. Beranek, L.L. Precision measurement of acoustic impedance. *J. Acoust. Soc. Am.* **1940**, *12*, 3–13. [CrossRef]
5. Taylor, K. Absolute calibration of microphones by a laser-Doppler technique. *J. Acoust. Soc. Am.* **1981**, *70*, 939–945. [CrossRef]
6. Zwikker, C.; Kosten, C.W. *Sound Absorbing Materials*; Elsevier Publishing Company: Amsterdam, The Netherlands, 1949.
7. Lanoye, R.; Boeckx, L.; De Geetere, L.; Vermeir, G.; Lauriks, W. Experience with different free field techniques to evaluate the surface impedance. In Proceedings of the 18th International Conference on Acoustics, Kyoto, Japan, 4–9 April 2004; pp. 1983–1986.
8. Alfarraj, M.; AlRegib, G. Semi-supervised learning for acoustic impedance inversion. In *SEG Technical Program Expanded Abstracts 2019*; Society of Exploration Geophysicists: Tulsa, OK, USA, 2019; pp. 2298–2302.
9. Di, H.; Chen, X.; Maniar, H.; Abubakar, A. Seismic acoustic impedance estimation by learning from sparse wells via deep neural networks. In Proceedings of the 82nd EAGE Annual Conference & Exhibition, European Association of Geoscientists & Engineers, Amsterdam, The Netherlands, 15 July 2020; Volume 2020, pp. 1–5. [CrossRef]
10. Nunes, R.; Azevedo, L.; Soares, A. Fast geostatistical seismic inversion coupling machine learning and Fourier decomposition. *Comput. Geosci.* **2019**, *23*, 1161–1172. [CrossRef]
11. Fuchs, H.; Möser, M. Sound absorbers. In *Handbook of Engineering Acoustics*; Springer: New York, NY, USA, 2013; pp. 165–214.
12. Sabine, P.E. The measurement of sound absorption coefficients. *J. Frankl. Inst.* **1929**, *207*, 341–368. [CrossRef]
13. Hodgson, M. When is diffuse-field theory applicable? *Appl. Acoust.* **1996**, *49*, 197–207. [CrossRef]
14. Young, R.W. Sabine reverberation equation and sound power calculations. *J. Acoust. Soc. Am.* **1959**, *31*, 912–921. [CrossRef]
15. Fitzroy, D. Reverberation formula which seems to be more accurate with nonuniform distribution of absorption. *J. Acoust. Soc. Am.* **1959**, *31*, 893–897. [CrossRef]
16. Arau-Puchades, H. An improved reverberation formula. *Acta Acust. United Acust.* **1988**, *65*, 163–180.
17. Neubauer, R.O. Estimation of reverberation time in rectangular rooms with non-uniformly distributed absorption using a modified Fitzroy equation. *Build. Acoust.* **2001**, *8*, 115–137. [CrossRef]
18. Schroeder, M.; Hackman, D. Iterative calculation of reverberation time. *Acta Acust. United Acust.* **1980**, *45*, 269–273.
19. Del Rey, R.; Alba, J.; Bertó, L.; Gregori, A. Small-sized reverberation chamber for the measurement of sound absorption. *Mater. Constr.* **2017**, *67*, 139. [CrossRef]
20. Acoustics—Measurement of Sound Absorption in a Reverberation Room. *ISO/TC 43/SC 2 Building Acoustics ISO 354:2003*. Available online: https://www.iso.org/standard/34545.html (accessed on 10 May 2021).
21. Acoustical Surfaces Inc. 2016. Available online: https://www.acousticalsurfaces.com/ (accessed on 10 May 2021).
22. Schultz, T. Diffusion in reverberation rooms. *J. Sound Vib.* **1971**, *16*, 17–28. [CrossRef]
23. West, J.C.; Bakore, R.; Bunting, C.F. Statistics of the current induced within a partially shielded enclosure in a reverberation chamber. *IEEE Trans. Electromagn. Compat.* **2017**, *59*, 2014–2022. [CrossRef]
24. West, J.C.; Bunting, C.F. Effects of frequency stirring on reverberation chamber testing: An analysis as a radiation problem. *IEEE Trans. Electromagn. Compat.* **2019**, *61*, 1345–1352. [CrossRef]
25. Kim, K.H.; Jeon, J.Y. Effect of diffusion conditions on absorption performance of materials evaluated in reverberation chamber. *Sustainability* **2019**, *11*, 6651. [CrossRef]
26. Xiang, D.; Wang, Z.; Chen, J. Acoustic design of a reverberation chamber. *Appl. Acoust.* **1991**, *32*, 83–91.
27. Sun, H.; Li, Z.; Gu, C.; Xu, Q.; Chen, X.; Sun, Y.; Lu, S.; Martin, F. Metasurfaced reverberation chamber. *Sci. Rep.* **2018**, *8*, 1–10.
28. Wanderlinder, L.F.; Lemaire, D.; Coccato, I.; Seetharamdoo, D. Practical implementation of metamaterials in a reverberation chamber to reduce the LUF. In Proceedings of the 2017 IEEE 5th International Symposium on Electromagnetic Compatibility (EMC-Beijing), IEEE, Beijing, China, 28–31 October 2017; pp. 1–3.
29. Zhao, J.; Li, X.; Wang, Y.; Wang, W.; Zhang, B.; Gai, X. Membrane acoustic metamaterial absorbers with magnetic negative stiffness. *J. Acoust. Soc. Am.* **2017**, *141*, 840–846. [CrossRef]
30. Noise, I.S. Acoustics—Determination of Sound Power Levels and Sound Energy Levels of Noise Sources Using Sound Pressure—Precision Methods for Reverberation Test Rooms. *ISO* **2010**. Available online: https://www.iso.org/about-us.html (accessed on 10 May 2021).
31. Nolan, M.; Jeong, C.H.; Brunskog, J.; Rodenas, J.; Chevillotte, F.; Jaouen, L. Different radiation impedance models for finite porous absorbers. *Proc. EuroNoise* **2015**. Available online: https://www.semanticscholar.org/paper/Different-Radiation-Impedance-Models-for-Finite-Nolan-Jeong/c2449d9021e286607859ed6655ece31f3694c267 (accessed on 10 May 2021).

32. Willardson, M.L.; Anderson, B.E.; Young, S.M.; Denison, M.H.; Patchett, B.D. Time reversal focusing of high amplitude sound in a reverberation chamber. *J. Acoust. Soc. Am.* **2018**, *143*, 696–705. [CrossRef]
33. Schroeder, M.R. New method of measuring reverberation time. *J. Acoust. Soc. Am.* **1965**, *37*, 1187–1188. [CrossRef]
34. Wen, J.Y.; Habets, E.A.; Naylor, P.A. Blind estimation of reverberation time based on the distribution of signal decay rates. In Proceedings of the 2008 IEEE International Conference on Acoustics, Speech and Signal Processing, IEEE, Las Vegas, NV, USA, 31 March–4 April 2008; pp. 329–332.
35. Nutter, D.B.; Leishman, T.W.; Sommerfeldt, S.D.; Blotter, J.D. Measurement of sound power and absorption in reverberation chambers using energy density. *J. Acoust. Soc. Am.* **2007**, *121*, 2700–2710. [CrossRef]
36. Clegg, J.; Marvin, A.C.; Dawson, J.F.; Porter, S.J. Optimization of stirrer designs in a reverberation chamber. *IEEE Trans. Electromagn. Compat.* **2005**, *47*, 824–832. [CrossRef]
37. Jones, M.G.; Stiede, P.E. Comparison of methods for determining specific acoustic impedance. *J. Acoust. Soc. Am.* **1997**, *101*, 2694–2704. [CrossRef]
38. Fahy, F. Rapid method for the measurement of sample acoustic impedance in a standing wave tube. *J. Sound Vib.* **1984**, *97*, 168–170. [CrossRef]
39. Chu, W. Single-microphone method for certain applications of the sound intensity technique. *J. Acoust. Soc. Am.* **1985**, *78*, S60. [CrossRef]
40. Chu, W.T. Transfer function technique for impedance and absorption measurements in an impedance tube using a single microphone. *J. Acoust. Soc. Am.* **1986**, *80*, 555–560. [CrossRef]
41. Singh, R. Acoustic impedance measurement methods. *Shock Vib. Inf. Center Shock Vib. Digest* **1982**, *14*, 3–10. [CrossRef]
42. Seybert, A.F.; Ross, D.F. Experimental determination of acoustic properties using a two-microphone random-excitation technique. *J. Acoust. Soc. Am.* **1977**, *61*, 1362–1370. [CrossRef]
43. Chung, J.; Blaser, D. Transfer function method of measuring in-duct acoustic properties. I. Theory. *J. Acoust. Soc. Am.* **1980**, *68*, 907–913. [CrossRef]
44. Chung, J.; Blaser, D. Transfer function method of measuring in-duct acoustic properties. II. Experiment. *J. Acoust. Soc. Am.* **1980**, *68*, 914–921. [CrossRef]
45. Schlieper, R.; Li, S.; Peissig, J. Development and Validation of a Full Range Acoustic Impedance Tube. In *Audio Engineering Society Convention 144*; Audio Engineering Society: New York, NY, USA, 2018.
46. Tan, W.H.; Ahmad, R.; Zunaidi, N.H.; Daud, R.; Cheng, E. Development of an indigenous impedance tube. *Appl. Mech. Mater. Trans. Tech. Publ.* **2015**, *786*, 149–155. [CrossRef]
47. Niresh, J.; Neelakrishnan, S.; Rani, S.S. Investigation and correction of error in impedance tube using intelligent techniques. *J. Appl. Res. Technol.* **2016**, *14*, 405–414. [CrossRef]
48. Fujimori, T.; Sato, S.; Miura, H. An automated measurement system of complex sound pressure reflection coefficients. In *INTER-NOISE and NOISE-CON Congress and Conference Proceedings*; Institute of Noise Control Engineering: Reston, Virginia, USA, 1984; Volume 1984, pp. 1009–1014.
49. Jones, M.G.; Parrott, T.L. Evaluation of a multi-point method for determining acoustic impedance. *Mech. Syst. Signal Process.* **1989**, *3*, 15–35. [CrossRef]
50. Cheung, W.S.; Jho, M.J.; Kim, Y.H. Improved method for the measurement of acoustic properties of a sound absorbent sample in the standing wave tube. *J. Acoust. Soc. Am.* **1995**, *97*, 2733–2739. [CrossRef]
51. de Bree, H.E. The Microflown, a New Particle Velocity Sensor. *Sound Vib.* **2005**, *39*, 8.
52. Ingård, U.; Bolt, R. A free field method of measuring the absorption coefficient of acoustic materials. *J. Acoust. Soc. Am.* **1951**, *23*, 509–516. [CrossRef]
53. Cremer, L. Bestimmung des Schallschluckgrads bei schrägem Schalleinfall mit Hilfe stehender Wellen. *Elektr. Nachr.-Techn. Bd* **1933**, *10*, 302.
54. Ando, Y. Interference-Pattern Method of Measuring Complex Reflection Coefficient of Acoustic Materials at Oblique Incidence. *Electron. Commun. Jpn.* **1968**, *51*, 10.
55. Sides, D. Absorption of Sound by Porous Fibrous Absorbents. Ph.D. Thesis, University of Liverpool, Liverpool, UK, 1973.
56. Sides, D.; Mulholland, K. The variation of normal layer impedance with angle of incidence. *J. Sound Vib.* **1971**, *14*, 139–142. [CrossRef]
57. Kintsl, Z. Investigation of Sound-Absorption of Wall Sections by a Pulse Technique. *Sov. Phys. Acoust.-USSR* **1975**, *21*, 30–32.
58. Yuzawa, M. A method of obtaining the oblique incident sound absorption coefficient through an on-the-spot measurement. *Appl. Acoust.* **1975**, *8*, 27–41. [CrossRef]
59. Hollin, K.; Jones, M. The measurement of sound absorption coefficient in situ by a correlation technique. *Acta Acust. United Acust.* **1977**, *37*, 103–110.
60. Richard, A.; Fernandez-Grande, E.; Brunskog, J.; Jeong, C.H. Estimation of surface impedance at oblique incidence based on sparse array processing. *J. Acoust. Soc. Am.* **2017**, *141*, 4115–4125. [CrossRef] [PubMed]
61. Dalmont, J.P. Acoustic impedance measurement, Part II: A new calibration method. *J. Sound Vib.* **2001**, *243*, 441–459. [CrossRef]
62. Benade, A.; Ibisi, M. Survey of impedance methods and a new piezo-disk-driven impedance head for air columns. *J. Acoust. Soc. Am.* **1987**, *81*, 1152–1167. [CrossRef]

63. Amédin, C.K.; Champoux, Y.; Berry, A. Acoustical characterization of absorbing porous materials through transmission measurements in a free field. *J. Acoust. Soc. Am.* **1997**, *102*, 1982–1994. [CrossRef]

64. Ren, M.; Jacobsen, F. A method of measuring the dynamic flow resistance and reactance of porous materials. *Appl. Acoust.* **1993**, *39*, 265–276. [CrossRef]

65. Takahashi, Y.; Otsuru, T.; Tomiku, R. In situ measurements of surface impedance and absorption coefficients of porous materials using two microphones and ambient noise. *Appl. Acoust.* **2005**, *66*, 845–865. [CrossRef]

66. Dickinson, P.J. Free Field Measurement of the Normal Acoustic Impedance of Ground Surfaces. Ph.D. Thesis, University of Southampton, Southampton, UK, 1968.

67. Embleton, T.F.; Piercy, J.E.; Daigle, G.A. Effective flow resistivity of ground surfaces determined by acoustical measurements. *J. Acoust. Soc. Am.* **1983**, *74*, 1239–1244. [CrossRef]

68. Allard, J.F.; Aknine, A.; Depollier, C. Acoustical properties of partially reticulated foams with high and medium flow resistance. *J. Acoust. Soc. Am.* **1986**, *79*, 1734–1740. [CrossRef]

69. Allard, J.; Delage, P. Free field measurements of absorption coefficients on square panels of absorbing materials. *J. Sound Vib.* **1985**, *101*, 161–170. [CrossRef]

70. Allard, J.; Depollier, C.; Guignouard, P. Free field surface impedance measurements of sound-absorbing materials with surface coatings. *Appl. Acoust.* **1989**, *26*, 199–207. [CrossRef]

71. Allard, J.F.; Champoux, Y.; Nicolas, J. Pressure variation above a layer of absorbing material and impedance measurement at oblique incidence and low frequencies. *J. Acoust. Soc. Am.* **1989**, *86*, 766–770. [CrossRef]

72. Allard, J.F.; Lauriks, W.; Verhaegen, C. The acoustic sound field above a porous layer and the estimation of the acoustic surface impedance from free-field measurements. *J. Acoust. Soc. Am.* **1992**, *91*, 3057–3060. [CrossRef]

73. Allard, J.; Aknine, A. Acoustic impedance measurements with a sound intensity meter. *Appl. Acoust.* **1985**, *18*, 69–75. [CrossRef]

74. Allard, J.; Bourdier, R.; L'Esperance, A. Anisotropy effect in glass wool on normal impedance in oblique incidence. *J. Sound Vib.* **1987**, *114*, 233–238. [CrossRef]

75. Allard, J.F.; Depollier, C.; Guignouard, P.; Rebillard, P. Effect of a resonance of the frame on the surface impedance of glass wool of high density and stiffness. *J. Acoust. Soc. Am.* **1991**, *89*, 999–1001. [CrossRef]

76. Allard, J.F.; Herzog, P.; Lafarge, D.; Tamura, M. Recent topics concerning the acoustics of fibrous and porous materials. *Appl. Acoust.* **1993**, *39*, 3–21. [CrossRef]

77. Allard, J.F.; Henry, M.; Gareton, V.; Jansens, G.; Lauriks, W. Impedance measurements around grazing incidence for nonlocally reacting thin porous layers. *J. Acoust. Soc. Am.* **2003**, *113*, 1210–1215. [CrossRef]

78. Champoux, Y.; Nicolas, J.; Allard, J. Measurement of acoustic impedance in a free field at low frequencies. *J. Sound Vib.* **1988**, *125*, 313–323. [CrossRef]

79. Champoux, Y.; L'espérance, A. Numerical evaluation of errors associated with the measurement of acoustic impedance in a free field using two microphones and a spectrum analyzer. *J. Acoust. Soc. Am.* **1988**, *84*, 30–38. [CrossRef]

80. Lafarge, D.; Allard, J.F.; Brouard, B.; Verhaegen, C.; Lauriks, W. Characteristic dimensions and prediction at high frequencies of the surface impedance of porous layers. *J. Acoust. Soc. Am.* **1993**, *93*, 2474–2478. [CrossRef]

81. Hutchinson-Howorth, C.; Attenborough, K.; Heap, N.W. Indirect in situ and free-field measurement of impedance model parameters or surface impedance of porous layers. *Appl. Acoust.* **1993**, *39*, 77–117. [CrossRef]

82. Daigle, G.; Stinson, M.R. Impedance of grass-covered ground at low frequencies measured using a phase difference technique. *J. Acoust. Soc. Am.* **1987**, *81*, 62–68. [CrossRef]

83. Legouis, T.; Nicolas, J. Phase gradient method of measuring the acoustic impedance of materials. *J. Acoust. Soc. Am.* **1987**, *81*, 44–50. [CrossRef]

84. Furstoss, M.; Thenail, D.; Galland, M.A. Surface impedance control for sound absorption: Direct and hybrid passive/active strategies. *J. Sound Vib.* **1997**, *203*, 219–236. [CrossRef]

85. Guicking, D.; Karcher, K. Active impedance control for one-dimensional sound. *J. Vib. Acoust. Stress Reliab. Des.* **1984**, *106*, 393–396. [CrossRef]

86. Glaretas, C. *A New Method for Measuring the Acoustic Impedance of the Ground*; The Pennsylvania State University: State College, PA, USA, 1981.

87. Glaretas, C. The free-field two-microphone method for the measurement of the acoustic impedance of the ground. *J. Acoust. Soc. Am.* **1982**, *72*, S88. [CrossRef]

88. Mommertz, E. Angle-dependent in-situ measurements of reflection coefficients using a subtraction technique. *Appl. Acoust.* **1995**, *46*, 251–263. [CrossRef]

89. Sugahara, A.; Lee, H.; Sakamoto, S.; Takeoka, S. Measurements of acoustic impedance of porous materials using a parametric loudspeaker with phononic crystals and phase-cancellation method. *Appl. Acoust.* **2019**, *152*, 54–62. [CrossRef]

90. Nocke, C. In-situ acoustic impedance measurement using a free-field transfer function method. *Appl. Acoust.* **2000**, *59*, 253–264. [CrossRef]

91. Nocke, C.; Mellert, V.; Waters-Fuller, T.; Attenborough, K.; Li, K. Impedance deduction from broad-band, point-source measurements at grazing incidence. *Acta Acust. United Acust.* **1997**, *83*, 1085–1090.

92. Nocke, C.; Mellert, V. *Brief Review on in situ Measurement Techniques of Impedance or Absorption*; Forum Acusticum: Sevilla, Spain, 2002.

93. Lam, G.C.; Leung, R.C.; Fan, H.K.; Aurégan, Y. Effect of back cavity configuration on performance of elastic panel acoustic liner with grazing flow. *J. Sound Vib.* **2021**, *492*, 115847. [CrossRef]

94. Dai, X.; Aurégan, Y. A cavity-by-cavity description of the aeroacoustic instability over a liner with a grazing flow. *J. Fluid Mech.* **2018**, *852*, 126–145. [CrossRef]

95. Bianco, F.; Fredianelli, L.; Lo Castro, F.; Gagliardi, P.; Fidecaro, F.; Licitra, G. Stabilization of a pu sensor mounted on a vehicle for measuring the acoustic impedance of road surfaces. *Sensors* **2020**, *20*, 1239. [CrossRef] [PubMed]

96. Praticò, F.; Vaiana, R.; Fedele, R. A study on the dependence of PEMs acoustic properties on incidence angle. *Int. J. Pavement Eng.* **2015**, *16*, 632–645.

97. Zuckerwar, A.J. Acoustic ground impedance meter. *J. Acoust. Soc. Am.* **1983**, *73*, 2180–2186. [CrossRef]

98. Jacobsen, F.; Liu, Y. Near field acoustic holography with particle velocity transducers. *J. Acoust. Soc. Am.* **2005**, *118*, 3139–3144. [CrossRef]

99. Jacobsen, F.; Jaud, V. A note on the calibration of pressure-velocity sound intensity probes. *J. Acoust. Soc. Am.* **2006**, *120*, 830–837. [CrossRef]

100. Hald, J.; Song, W.; Haddad, K.; Jeong, C.H.; Richard, A. In-situ impedance and absorption coefficient measurements using a double-layer microphone array. *Appl. Acoust.* **2019**, *143*, 74–83. [CrossRef]

101. Renou, Y.; Aurégan, Y. Failure of the Ingard–Myers boundary condition for a lined duct: An experimental investigation. *J. Acoust. Soc. Am.* **2011**, *130*, 52–60. [CrossRef] [PubMed]

102. Groby, J.P.; Huang, W.; Lardeau, A.; Aurégan, Y. The use of slow waves to design simple sound absorbing materials. *J. Appl. Phys.* **2015**, *117*, 124903. [CrossRef]

103. Guo, W.; Liu, J.; Bi, W.; Yang, D.; Aurégan, Y.; Pagneux, V. Spatial transient behavior in waveguides with lossy impedance boundary conditions. *arXiv* **2020**, arXiv:2010.03646.

104. Berardi, U.; Iannace, G. Predicting the sound absorption of natural materials: Best-fit inverse laws for the acoustic impedance and the propagation constant. *Appl. Acoust.* **2017**, *115*, 131–138. [CrossRef]

105. Iannace, G.; Ianniello, C.; Maffei, L.; Romano, R. Steady-state air-flow and acoustic measurement of the resistivity of loose granular materials. *J. Acoust. Soc. Am.* **1999**, *106*, 1416–1419. [CrossRef]

106. Liu, C.; Luo, J.; Lai, Y. Acoustic metamaterials with broadband and wide-angle impedance matching. *Phys. Rev. Mater.* **2018**, *2*, 045201. [CrossRef]

107. Le Duff, A.; Plantier, G.; Valière, J.C.; Gazengel, B. Acoustic velocity measurement by means of Laser Doppler Velocimetry: Development of an Extended Kalman Filter and validation in free-field measurement. *Mech. Syst. Signal Process.* **2016**, *70*, 832–852. [CrossRef]

108. Merkl, J.; Hiremath, N.; Raghav, V.; Komerath, N. Extracting Static Pressure From Velocimetry in Vortical Flows. In *ASME/JSME/KSME 2015 Joint Fluids Engineering Conference*; American Society of Mechanical Engineers: New York, NY, USA, 2015; p. V001T20A001.